

The Dark Side of the Cosmos:

Exploring Dark Energy and Modified Gravity

CosmoVerse Conference 2025
@ (ITU, Istanbul, Turkey)

Mariam Bouhmadi-López
IKERBASQUE & EHU (Spain)



June 26th, 2025

Table of contents

1. Introduction
2. Speeding up with fields
3. Modified theory within $f(Q)$ gravity
4. Conclusions

Introduction

Introduction-1-: A brief sketch of the universe

- The universe is homogeneous and isotropic on large scales (cosmological principle)
- The matter content of the universe:
 - Standard matter
 - Dark matter
 - Something that induce the late-time acceleration of the Universe
- The acceleration of the universe is backed by several measurments: $H(z)$, Snela, BAO, CMB, LSS (matter power spectrum, growth function)...

- The **effective** equation of state of whatever is driving the current speed up of the universe is roughly -1 .
- Such an acceleration could be due to:
 - A new component of the energy budget of the universe: dark energy; i.e. it could be Λ (i.e. a non dynamical dark energy), quintessence, of a phantom(-like/effective) nature
 - A change on the behaviour of gravity on the largest scale. No new component on the budget of the universe but rather simply gravity modifies its behaviour, within a metric, Palatini (affine metric), in presence of torsion or non-metricity

Cosmological problems

- If Λ is driving the current acceleration of the Universe, then:
 - Coincidence problem. How is this sensible to initial conditions?
 - Why now? Dark energy seems to be dominant only at late-time, not before.
 - Fine-tuning problem. New energetic scale $\rho_\Lambda \approx 10^{-47} \text{ GeV}^4$. It is very small compared to other scales.
 - Cosmological tensions, in particular the Hubble tension.
- How might evolving dark energy models or extended theories of gravity help to address the issues discussed above?

Speeding up with fields

Speeding up with fields

Quintessence through a generalised axion-like potential

Quintessence

- Minimally coupled canonical scalar field:

$$L = \frac{1}{2k^2}R - \frac{1}{2}g^{\mu\nu}\nabla_\mu\phi\nabla_\nu\phi - V(\phi) + L_{r,m}.$$

- ϕ is a dynamical field.
- Coincidence problem.** It can be alleviated by scaling solutions and tracker fields.
- Fine-tuning problem remains unsolved.
- Some quintessence models allow for a natural explanation of why now?
 - Could the tensions H_0 and S_8 been alleviated?
- An axion-like potential: $V(\phi) = \Lambda^4[1 - \cos(\phi/\eta)]^{-n}$ with a generalisation to **negative exponents, i.e. $0 < n$** .
- Previously analysed on the context of wave dark matter and early dark energy [Wave Dark Matter](#) (L. Hui). [arXiv:2101.11735], [Dark energy from the string axiverse](#) (M. Kamionkowski). [arXiv:1409.0549]

Dynamical system

- Dynamical variables (FLRW filled by rad., mat. and an axion-like field):

$$x = \frac{k\dot{\phi}}{\sqrt{6}H}, \quad y = \frac{k\sqrt{V}}{\sqrt{3}H}, \quad \lambda = -\frac{V_{,\phi}}{kV}, \quad z = \Omega_r^{1/2} = \frac{k\sqrt{\rho_r}}{\sqrt{3}H}.$$

- Matter part: $\Omega_m = 1 - x^2 - y^2 - z^2$.
- Autonomous closed system of equations:

$$x' = \frac{1}{2} [-3x + 3x^3 - 3xy^2 + xz^2] + \sqrt{\frac{3}{2}}\lambda y^2,$$

$$y' = \frac{1}{2} [3y - 3y^3 + 3yx^2 + yz^2] - \sqrt{\frac{3}{2}}\lambda xy,$$

$$z' = \frac{1}{2} [-z + z^3 + 3zx^2 - 3zy^2],$$

$$\lambda' = -\sqrt{6}f(\lambda)x, \quad f(\lambda) = \lambda^2[\Gamma(\lambda) - 1], \quad \Gamma = \frac{V_{,\phi\phi}V}{(V_{,\phi})^2}$$

Fixed points

Point	x	y	z	λ	w_{eff}	Stability
A_1	0	0	0	Any	0	Saddle
A_2	0	0	1	Any	$1/3$	Saddle
E	0	1	0	0	-1	(Un)Stable if $n > 0$ ($n < 0$)

Tracking behaviour

Unique evolution of ϕ . It does not depend on the initial conditions.

Tracking regime given by $\omega_\phi \approx \text{const}$.

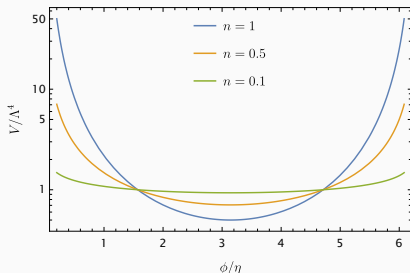
- Tracking with $\omega_\phi > \omega$: it could happen, but it is disregarded (structure formation suppression). Here ω stands for EoS of radiation or matter.
- **Tracking with $\omega_\phi < \omega$: $\Gamma > 1$ and $\Gamma \approx \text{const}$. in the regime $\lambda \gg 1$.**

$$\omega_\phi = \frac{\omega - 2(\Gamma - 1)}{1 + 2(\Gamma - 1)}.$$

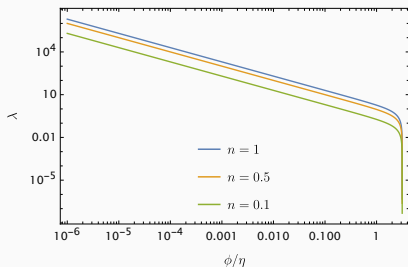
Axion-like potential

$$V(\phi) = \Lambda^4 [1 - \cos(\phi/\eta)]^{-n}.$$

Generalisation to $n > 0$



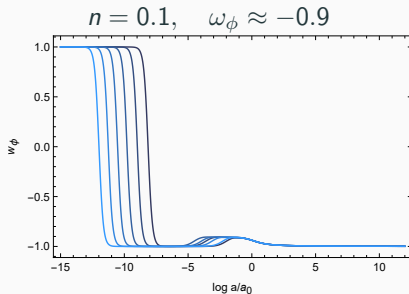
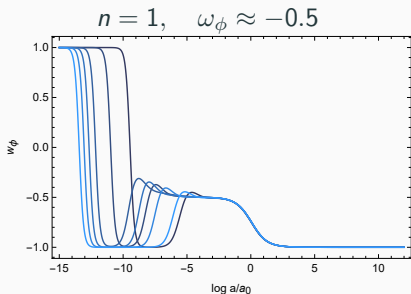
$$\lambda(\phi) = \frac{n}{k\eta} \frac{\sin(\phi/\eta)}{1 - \cos(\phi/\eta)}$$



- Cosmological constant in the limit $n \rightarrow 0$.
- Minimum at $\phi/\eta = \pi \rightarrow V \approx V_{\min} + \frac{1}{2}m^2(\phi - \pi\eta)^2$ where $V_{\min} \equiv \Lambda^4/2^n$ and $m^2 \equiv n\Lambda^4/(2^{n+1}\eta^2)$.
- $\phi_{ini}/\eta \ll 1$ in order to have non-trivial evolution $\rightarrow \lambda_{ini} \gg 1$.

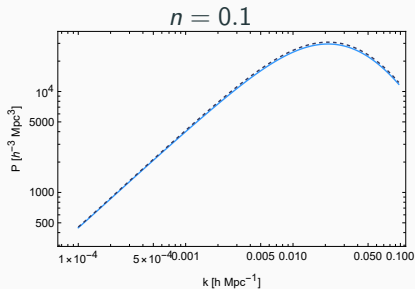
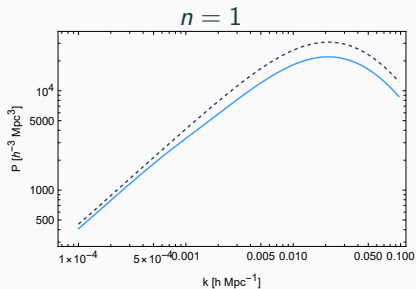
Fixed points and tracking

- Fixed points: A_1 , A_2 and E (minimum of the potential). E is an attractor \rightarrow **Late-time acceleration**.
- $\Gamma(\lambda) = 1 + \frac{1}{2n} + \frac{n}{2k^2\eta^2\lambda^2}$. In the regime $\lambda \gg 1$: $\Gamma \approx 1 + \frac{1}{2n} \rightarrow$ **Tracking behaviour** with $\omega_\phi < \omega$.
- Tracking regime given by $\omega_\phi \approx -\frac{2(\Gamma-1)}{1+2(\Gamma-1)} = -\frac{1}{1+n}$ ($\omega = 0$).

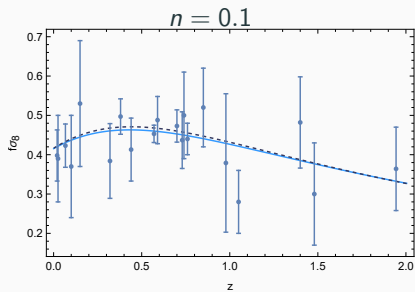
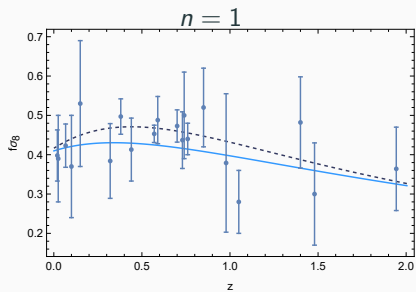


Matter power spectrum

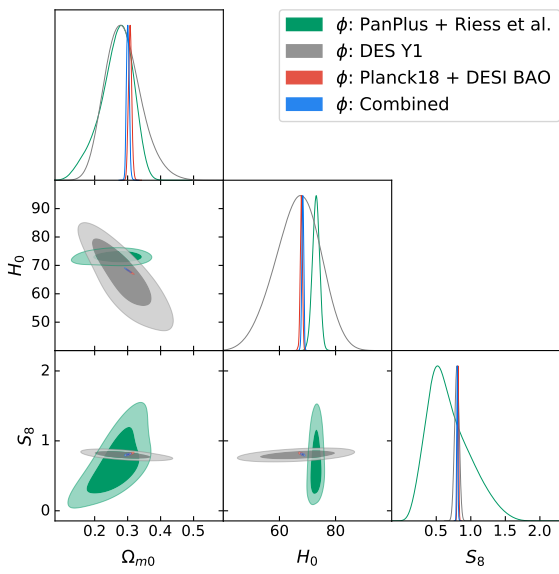
Matter power spectrum suppression:



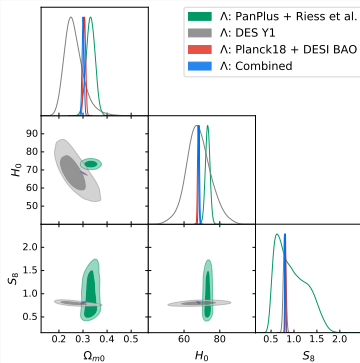
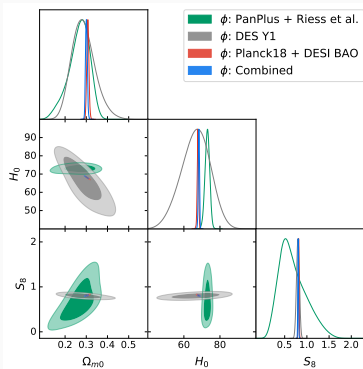
$f\sigma_8$ distribution:



Fitting the model-1-



Comparing the model



Fitting the model-2-

	CMB	+ BAO	+ SNe	+ low-z	+ DES Y1
$10^3 \Omega_b h^2$	22.19 ± 0.13	22.29 ± 0.12	22.26 ± 0.12	22.34 ± 0.12	22.38 ± 0.12
$10^3 \Omega_c h^2$	119.7 ± 1.0	118.26 ± 0.81	118.56 ± 0.79	117.80 ± 0.76	117.27 ± 0.72
$10^3 \theta_{MC}$	1040.77 ± 0.25	1040.94 ± 0.24	1040.91 ± 0.24	1041.01 ± 0.24	1041.05 ± 0.24
$\ln(10^{10} A_s)$	3.037 ± 0.014	3.044 ± 0.014	3.043 ± 0.014	3.047 ± 0.014	3.046 ± 0.014
n_s	0.9636 ± 0.0040	0.9672 ± 0.0036	0.9665 ± 0.0036	0.9685 ± 0.0036	0.9693 ± 0.0036
τ_{reio}	0.0524 ± 0.0071	0.0571 ± 0.0071	0.0562 ± 0.0070	0.0587 ± 0.0071	0.0589 ± 0.0071
H_0	67.24 ± 0.46	67.89 ± 0.36	67.76 ± 0.35	68.12 ± 0.34	68.36 ± 0.32
Ω_{m0}	0.3154 ± 0.0064	0.3064 ± 0.0048	0.3082 ± 0.0047	0.3034 ± 0.0044	0.3003 ± 0.0042
σ_8	0.8077 ± 0.0055	0.8064 ± 0.0056	0.8067 ± 0.0056	0.8061 ± 0.0057	0.8041 ± 0.0055
S_8	0.828 ± 0.011	0.8149 ± 0.0090	0.8176 ± 0.0090	0.8107 ± 0.0087	0.8044 ± 0.0080
DIC	5497.90 ± 0.12	5507.21 ± 0.37	6209.34 ± 0.14	6217.77 ± 0.43	6477.38 ± 0.28
WAIC	5499.09 ± 0.50	5507.85 ± 0.18	6210.36 ± 0.21	6218.68 ± 0.21	6481.16 ± 0.22
$-\ln B$	5499.3 ± 1.1	5508.13 ± 0.73	6210.51 ± 0.44	6219.1 ± 1.4	6479.9 ± 1.2

Table 2. Mean and standard deviation of cosmological parameters, late-time observables, and statistical probes for Λ CDM model. From left to right are gradually larger datasets that progressively add in datasets of CMB, BAO, etc., as defined in section 3.1.

	CMB	+ BAO	+ SNe	+ low-z	+ DES Y1
$10^4 \Omega_b h^2$	22.18 ± 0.13	22.28 ± 0.12	22.28 ± 0.12	22.34 ± 0.12	22.39 ± 0.12
$10^4 \Omega_c h^2$	119.8 ± 1.1	118.29 ± 0.80	118.40 ± 0.83	117.73 ± 0.79	117.22 ± 0.73
$10^3 \theta_{MC}$	1040.76 ± 0.25	1040.95 ± 0.24	1040.93 ± 0.24	1041.03 ± 0.23	1041.06 ± 0.26
$\ln(10^{10} A_s)$	3.039 ± 0.014	3.044 ± 0.014	3.044 ± 0.014	3.048 ± 0.014	3.048 ± 0.014
n_s	0.9634 ± 0.0040	0.9671 ± 0.0036	0.9669 ± 0.0037	0.9686 ± 0.0036	0.9694 ± 0.0035
τ_{reio}	0.0532 ± 0.0071	0.0568 ± 0.0073	0.0566 ± 0.0071	0.0590 ± 0.0072	0.0596 ± 0.0073
$\log_{10}(\rho_{DE,0}/V_{min} - 1)$	$-2.9^{+2.1}_{-0.7}$	$-2.92^{+0.49}_{-0.75}$	$-3.0^{+2.9}_{-0.6}$	$-2.94^{+0.43}_{-0.76}$	$-3.0^{+3.1}_{-0.8}$
$\log_{10}(\eta/M_P)$	$-1.25^{+0.31}_{-0.6}$	$0^{+0.6}_{-0.5}$	$-2.0^{+1.5}_{-0.5}$	$0^{+0.6}_{-0.6}$	$-2.0^{+1.7}_{-0.8}$
α	$0.5^{+3.3}_{-3.3}$	$0.5^{+3.8}_{-3.8}$	$0.5^{+2.6}_{-2.6}$	$0.5^{+2.6}_{-2.6}$	$0.5^{+1.2}_{-1.2}$
$\log_{10}(\phi_s/\eta)$	$67.05^{+0.92}_{-0.97}$	67.77 ± 0.39	67.62 ± 0.45	68.08 ± 0.36	68.31 ± 0.33
H_0	$0.3177^{+0.0065}_{-0.0078}$	0.3075 ± 0.0049	0.3091 ± 0.0053	0.3036 ± 0.0046	0.3006 ± 0.0042
Ω_{m0}	$0.8056^{+0.0070}_{-0.0079}$	0.8049 ± 0.0062	0.8042 ± 0.0067	0.8052 ± 0.0059	0.8035 ± 0.0059
σ_8	0.831 ± 0.012	0.8149 ± 0.0091	0.8163 ± 0.0090	0.8100 ± 0.0089	0.8042 ± 0.0080
DIC	5498.13 ± 0.54	5507.87 ± 0.13	6210.08 ± 0.35	6218.58 ± 0.01	6478.21 ± 0.53
WAIC	5499.03 ± 0.53	5508.42 ± 0.15	6210.85 ± 0.03	6219.12 ± 0.29	6481.97 ± 0.92
$-\ln B$	5499.74 ± 0.99	5509.2 ± 2.4	6210.17 ± 0.04	6219.09 ± 0.20	6482.8 ± 2.8
Δ DIC	0.23 ± 0.59	0.66 ± 0.41	0.74 ± 0.39	0.81 ± 0.51	0.83 ± 0.63
Δ WAIC	-0.06 ± 0.77	0.56 ± 0.24	0.48 ± 0.45	0.43 ± 0.39	0.81 ± 0.97
$-\Delta \ln B$	0.4 ± 1.6	1.0 ± 2.4	-0.35 ± 0.52	-0.1 ± 1.7	2.9 ± 3.2

Table 3. Mean and standard deviation of cosmological parameters, late-time observables, and statistical probes for the axion-like dark energy model in section 2. From left to right are gradually larger datasets of CMB, CMB + BAO, CMB + BAO + SNe, etc., as defined in section 3.1. Δ ICs are with respect to Λ CDM model presented in table 2. For parameters not following Gaussian distribution we provide the median and 68% lower and upper bounds (if valid) instead, with color coding for how heavy the tail is (red for short tail, black for Gaussian, blue for exponential, and cyan for long tail.) For single-sided distributions we report the modal and the single-sided 68% bound instead.

	BAO	SNe + low-z	DES Y1
$10^3 \Omega_c h^2$	111 ± 11	116 ± 29	107^{+15}_{-19}
$10^5 \theta_{MC}$	1036 ± 12	1081^{+15}_{-18}	1048^{+36}_{-38}
$\ln(10^{10} A_s)$			$3.47^{+0.27}_{-0.29}$
$\log(\rho_{DE,0}/V_{\min} - 1)$	$-2.8^{+2.1}_{-0.6}$	$-0.08^{+0.80}_{-0.95}$	$-1.0^{+1.3}_{-1.6}$
$\log(\eta/M_P)$	$-0.89^{+0.56}$	$0.5^{+1.0}_{-0.5}$	$-0.3^{+1.0}_{-0.4}$
n	0.4	$0^{+0.5}$	0.4
$\log(\phi_i/\eta)$	$0.5^{+1.0}_{-3.2}$	-1.4	$0.5^{+1.3}_{-2.9}$
H_0	$68.5^{+1.0}_{-1.4}$	73.0 ± 1.3	70.4 ± 5.5
Ω_{m0}	0.291 ± 0.016	$0.281^{+0.043}_{-0.053}$	0.266 ± 0.046
σ_8			0.862 ± 0.093
S_8			0.802 ± 0.031
DIC	8.53 ± 0.12	703.54 ± 0.33	260.86 ± 0.72
WAIC	8.26 ± 0.21	703.40 ± 0.45	262.36 ± 0.68
$-\ln B$	8.33 ± 0.26	703.56 ± 0.11	262.26 ± 0.29
Δ DIC	0.08 ± 0.14	0.17 ± 0.34	0.2 ± 1.1
Δ WAIC	-0.24 ± 0.27	0.09 ± 0.46	-0.27 ± 0.69
$-\Delta \ln B$	-0.53 ± 0.48	0.07 ± 0.17	-0.10 ± 0.98
Tension against	CMB	CMB + BAO	CMB + BAO + SNe + low-z
R	1.2 ± 2.8	6.3 ± 2.8	1.5 ± 2.8
GoF	$2.33 \pm 0.25\sigma$	$4.20 \pm 0.23\sigma$	$2.93 \pm 0.35\sigma$
S	$2.08 \pm 0.41\sigma$	$3.96 \pm 0.26\sigma$	$1.86 \pm 0.47\sigma$
ΔR	1.2 ± 3.1	-1.2 ± 3.2	3.1 ± 3.5
Δ GoF	$0.39 \pm 0.39\sigma$	$-0.10 \pm 0.30\sigma$	$0.39 \pm 0.46\sigma$
ΔS	$0.40 \pm 0.45\sigma$	$-0.10 \pm 0.31\sigma$	$0.26 \pm 0.48\sigma$

Table 6. Mean and standard deviation of cosmological parameters, late-time observables, and statistical probes for the axion-like dark energy model in section 2. From left to right are datasets of BAO, SNe + low-z, and DES Y1. Δ ICs and delta of tension probes are with respect to Λ CDM model presented in table 5. Tension probes of $-\ln R$, GoF and S are with respect to axion-like dark energy model inside table 4 according to “Tension against” row. For parameters not following Gaussian distribution we provide the median and 68% lower and upper bounds (if valid) instead, with colour coding for how heavy the tail is (red for short tail, black for Gaussian, blue for exponential, and cyan for long tail.) If the distribution is clearly single-sided we report the modal and the single-sided 68% bound instead.

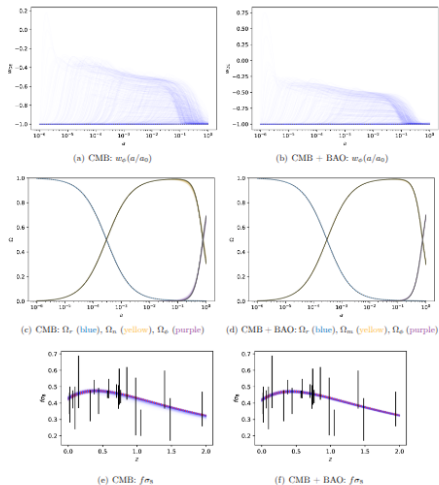
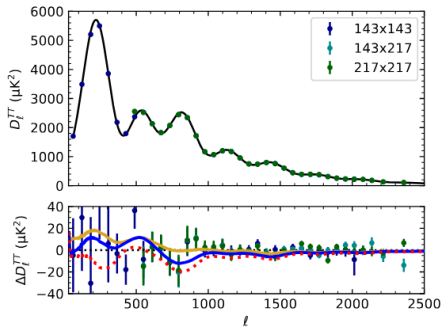


Figure 8. The dark energy equation of state w_0 (top), density parameters (centre) of radiation Ω_r (blue), matter Ω_m (yellow) and dark energy Ω_b (purple) as functions of z for 600 samples drawn from individual fits. Left figures: Models fitted against CMB dataset. Right figures: Models fitted against CMB + BAO dataset. Black line denotes Λ CDM model and non-black lines denote the axion-like dark energy model. Without additional distance measurement, CMB dataset alone permits variation of the density parameter evolution as depicted in Fig. 2. However, once BAO dataset is included, the density parameters stabilise and the tracking regime has to end before $a/a_0 = 1$. In bottom figures, the $f\sigma_8$ data are taken from table 2 of [76].



(a) CMB TT power spectrum

Figure 9. The best fit CMB TT power spectrum (*top*) and the residue (*bottom*) against best fit Λ CDM model TT power spectrum of CMB dataset. *Top:* The best fit CMB TT power spectrum of Λ CDM model and the data from Planck CamSpec PR4 data release in Fig. 6 of [16]. *Bottom:* Black *dotted* line and red *dotted* line denote Λ CDM model fitted against CMB and CMB + BAO datasets respectively; and yellow *solid* line and blue *solid* line denotes axion-like dark energy model fitted against CMB and CMB + BAO datasets respectively. There are no visible difference between two models.

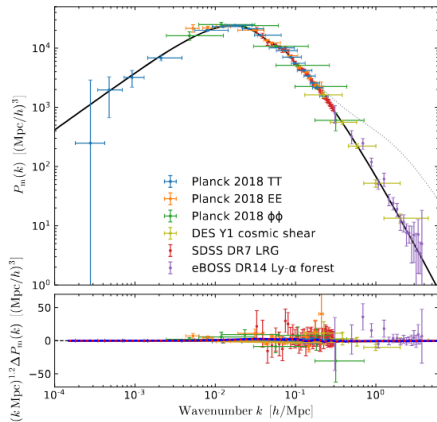


Figure 11. The best fit matter power spectrum (*top*) and the residue (*bottom*) against best fit Λ CDM model matter power spectrum of CMB dataset. *Top:* *Solid* lines represents the linear power spectrum and the *dotted* lines represents the nonlinear power spectrum. Matter power spectrum data taken from Fig. 1 of [79]. *Bottom:* *Black dashed* line and *red dotted* line denote Λ CDM model fitted against CMB and CMB + BAO datasets respectively, and *yellow solid* line and *blue solid* line denotes axion-like dark energy model fitted against CMB and CMB + BAO datasets respectively. There are no visible difference between three best fit models.

Speeding up with fields

Late-time acceleration of the universe within Kinetic Gravity Braiding theories

Kinetic gravity Braiding theories

- The gravitational action (Deffayet, Pujolas, Sawiki and Vikman, arXiv: 1008.0048 [hep-th]. Published in JCAP 2010) :

$$S = \int d^4x \sqrt{-g} \left[\frac{1}{2} R + K(\phi, X) - G(\phi, X) \square \phi \right]$$

- Passes constraints from GR170817
- Essential mixing
- (Im)Perfect fluid
- Self-tuning de Sitter solution
- (Subdominant) Phantom behaviour without ghost nor gradient instabilities (where the equation of state of the scalar field < -1)
- We will assume the **shift-symmetric case: the action is invariant under $\phi \rightarrow \phi + c$** where c is a constant
- **Our goal is to analyse the future evolution of the shift-symmetric Kinetic Gravity Braiding theories and see if we can have dominant phantom behaviour without ghost and gradient instabilities.** (Borislavov,

Bouhmadi-López, and Martín-Moruno arXiv:2210.07276, 2212.02547, 2406.12576, PLB 2023, JCAP 2023, Phys. Dark Univ.

2024)

Background dynamics

- Conserved shift current: $J = \dot{\phi}K_X + 6XG_XH$
- Background gravitational equations:
 - Friedmann eq: $3H^2 = \rho_m + \rho_r - K + \dot{\phi}J$
 - Raychaudhuri eq: $\dot{H} = -\frac{1}{2}(\rho_m + \frac{4}{3}\rho_r) + XG_X\ddot{\phi} - \frac{1}{2}\dot{\phi}J$
- Conservation equations:
 - $\dot{\rho}_m = -3H\rho_m$
 - $\dot{\rho}_r = -4H\rho_r$
 - $\dot{J} = -3HJ$, therefore, $J = Q_0 \left(\frac{a}{a_0}\right)^{-3}$.

A dynamical system approach: **suitable** definition of the variables

- The matter dimensionless variables reads

$$\Omega_r := \frac{\rho_r}{3H^2},$$

$$\Omega_m := \frac{\rho_m}{3H^2},$$

$$\Omega_\phi := \frac{\epsilon\sqrt{2XJ - K}}{3H^2}$$

- We assume Ω_ϕ to be positive since we are mainly interested in the future attractors of expanding FLRW models. Hence, $\Omega_i \in [0, 1]$ for $i \in \{r, m, \phi\}$.
- We carry out our analysis for expanding solutions; i.e. H positive

$$\frac{H}{H_0} = \frac{h}{1 - h^2} \quad \longrightarrow \quad h \in [0, 1]$$

- Through the above definition we obtain new solutions that were overlooked previously.
- The Friedmann constraint reads: $\Omega_r + \Omega_m + \Omega_\phi = 1$

A dynamical system approach: evolution of the system

- Evolution:

$$\begin{aligned}h' &= \frac{(1-h^2)h}{1+h^2} C_1, \\ \Omega_r' &= -2\Omega_r (2 + C_1), \\ \Omega_\phi' &= C_2 - 2\Omega_\phi C_1,\end{aligned}$$

- Auxiliary functions:

$$C_1 := \frac{H'}{H}, \quad C_2 := \frac{\epsilon\sqrt{2X}}{H^2} (HG_X X' - J)$$

- Equations of state:

$$w_{\text{eff}} := \frac{P_{\text{tot}}}{\rho_{\text{tot}}} = -1 - \frac{2}{3} C_1, \quad w_\phi := \frac{P_\phi}{\rho_\phi} = -1 - \frac{1}{3\Omega_\phi} C_2.$$

- A prime stands for derivative respect to $\ln(a)$.

A dynamical system approach: fixed points

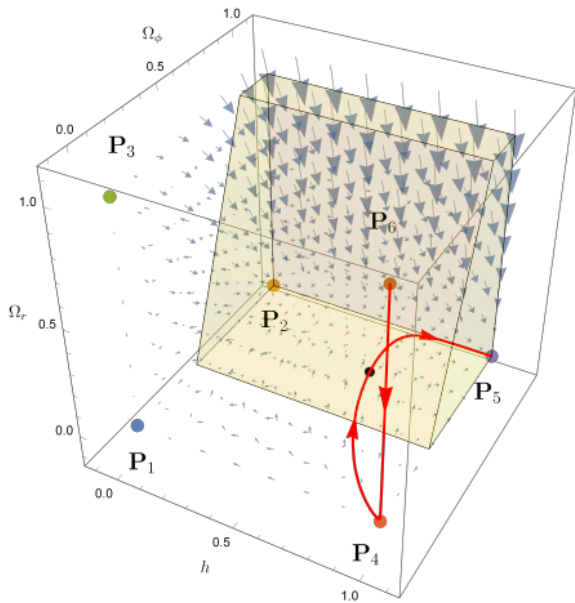
1. Vacuum solutions dominated by matter or the scalar field:
($h^{\text{fp}} = \Omega_r^{\text{fp}} = 0$, $C_1^{\text{fp}} \neq -2$ and $C_2^{\text{fp}} = 2C_1^{\text{fp}}\Omega_\phi^{\text{fp}}$)
2. Vacuum solutions where radiation like effects dominates the nearby evolution of the system, i.e. $w_{\text{eff}}^{\text{fp}} = 1/3$. Scaling solutions for the scalar field. ($h^{\text{fp}} = 0$, $C_1^{\text{fp}} = -2$ and $C_2^{\text{fp}} = -4\Omega_\phi^{\text{fp}}$):
3. Cosmological singularities (Ex. BR) ($h^{\text{fp}} = 1$, $\Omega_r^{\text{fp}} = 0$, $C_1^{\text{fp}} \neq -2$ and $C_2^{\text{fp}} = 2C_1^{\text{fp}}\Omega_\phi^{\text{fp}}$)
4. Initial cosmological singularities. It is a radiation dominated regime ($w_{\text{eff}}^{\text{fp}} = 1/3$). ($h^{\text{fp}} = 1$, $C_1^{\text{fp}} = -2$ and $C_2^{\text{fp}} = -4\Omega_\phi^{\text{fp}}$)
5. de Sitter solutions Ex. ($h^{\text{fp}} \neq \{0, 1\}$, $\Omega_r^{\text{fp}} = 0$ and $C_1^{\text{fp}} = C_2^{\text{fp}} = 0$):

Proxy model: $K(X) = 0$ and $G(X) = c_G X^\beta$

Fixed Point	$(h^{\text{fp}}, \Omega_\phi^{\text{fp}}, \Omega_r^{\text{fp}})$	w_ϕ^{fp}	$w_{\text{eff}}^{\text{fp}}$	$\beta < -\frac{1}{2}$	$\beta = -\frac{1}{2}$	$-\frac{1}{2} < \beta < -\frac{1}{4}$	$\beta = -\frac{1}{4}$	$-\frac{1}{4} < \beta < 0$	$0 < \beta < \frac{1}{2}$	$\beta = \frac{1}{2}$	$\frac{1}{2} < \beta$
P ₁ (vacuum)	(0, 0, 0)	$\frac{1}{4\beta}$	0	saddle	saddle	saddle	saddle	saddle	attractor	attractor	attractor
P ₂ (vacuum)	(0, 1, 0)	$\frac{1}{4\beta+1}$	$\frac{1}{4\beta+1}$	attractor	—	saddle	—	saddle	saddle	—	saddle
P ₃ (vacuum)	(0, 0, 1)	$\frac{1}{6\beta}$	$\frac{1}{3}$	saddle	saddle	saddle	saddle	saddle	saddle	—	saddle
P ₄ (BB)	(1, 0, 0)	$\frac{1}{4\beta}$	0	saddle	saddle	saddle	saddle	saddle	saddle	saddle	saddle
P ₅ (BB/BR)	(1, 1, 0)	$\frac{1}{4\beta+1}$	$\frac{1}{4\beta+1}$	saddle	—	attractor	—	repeller	repeller	—	saddle
P ₆ (BB)	(1, 0, 1)	$\frac{1}{6\beta}$	$\frac{1}{3}$	repeller	repeller	repeller	repeller	repeller	saddle	—	repeller
P ₇ (BF)	(1, 1, 0)	$-\infty$	$-\infty$	—	—	—	attractor*	—	—	—	—
L ₁ (dS)	$(h^{\text{fp}}, 1, 0)$	-1	-1	—	attractor	—	—	—	—	—	—
L ₂ (sudden)	$(h^{\text{fp}}, -4\beta, \Omega_r^{\text{fp}})$	$-\infty$	$-\infty$	—	—	—	—	attractor*	—	—	—
L ₃ (vacuum)	$(0, \Omega_\phi^{\text{fp}}, \Omega_r^{\text{fp}})$	$\frac{1}{3}$	$\frac{1}{3}$	—	—	—	—	—	—	saddle	—
L ₄ (BB)	$(1, \Omega_\phi^{\text{fp}}, \Omega_r^{\text{fp}})$	$\frac{1}{3}$	$\frac{1}{3}$	—	—	—	—	—	—	repeller	—

TABLE I. Classification and linear stability of the fixed points of our model. A superscript “fp” indicates evaluation at the fixed point. A horizontal bar denotes that the corresponding fixed point does not exist. The physical interpretation of each point is shown in brackets where BB stands for Big Bang and BF for Big Freeze. The labels L₁, L₂, L₃ and L₄ represent sets of non-isolated fixed points where h^{fp} can take any values. In addition, $\Omega_r^{\text{fp}} \in [0, 1 + 4\beta]$ holds for L₂, and $\Omega_\phi^{\text{fp}} + \Omega_r^{\text{fp}} = 1$ for L₃ and L₄. The starred quantities designate fixed points that have eluded our dynamical system analysis because of the choice of the dynamical variables but whose existence and stability follows directly from the Friedmann equations.

Proxy model: $K(X) = 0$ and $G(X) = c_G X^\beta$



Proxy model: $K(X) = 0$ and $G(X) = c_G X^\beta$

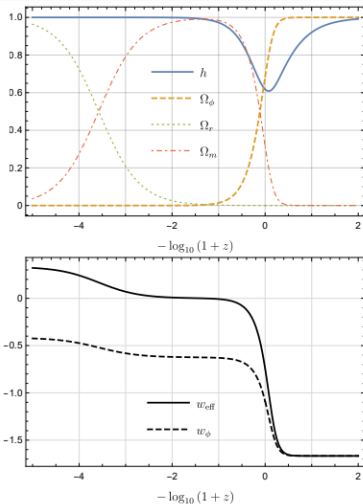


FIG. 2. Numerical evolution of the dynamical system (19)-(21) for $\beta = -2/5$ with the same initial conditions as in figure 1. Top panel: the variable h and the partial densities Ω_i for $i = \{m, r, \phi\}$. Bottom panel: the effective equation of state parameter w_{eff} and the equation of state parameter w_ϕ for the scalar field.

Stability of the system at the perturbative level

1. At zero order (background): the system is stable, i.e. there are attractor solutions.
2. At first order: (at least for the simplest model we have analysed) a **tachyonic** or a **ghost** issue can arise and they are complementary; i.e. if we avoid one, the other one shows up. We think the tachyonic one is more problematic as it can affect the large scale structure. The other one can be shown to be avoided when quantising gravity and the matter fields (WdW approach).
3. At second order: the scalar perturbations could feed an overproduction of gravitational waves.

Speeding up with fields

Late-time acceleration through a 3-form field

Can we have something beyond scalar fields to describe DE?

- Can we have something beyond scalar fields to describe DE?
 - A possibility come in the form of 3-forms.
 - Inspired in supergravity and string theory: Aurilia, Nicolai, Townsend (1980), Copeland, Lahiri, Wands (1995)
 - Massless 3-form as Cosmological Constant (solving CC problem): Turok, Hawking (1998)
 - Inflation or late time acceleration driven by self-interacting 3-forms: Koivisto, Nunes (2009) and (2010)
 - Non-Gaussianity: Kumar, Mulryne, Nunes, Marto, Moniz (2016)
 - Quantum cosmology with 3-forms: Bouhmadi-López, Brizuela, Garay (2018)
 - DE models (quintessence like and phantom as well): Morais, Bouhmadi-López, Kumar, Marto, Tavakoli, Phys. Dark Univ., arXiv: 1608.01679 , Bouhmadi-López, Marto, Morais and Silva, JCAP, arXiv: 1611.03100 M.B.-L, H.-W. Chiang, C.G. Boiza and P. Chen: work in progress (the observational fit)

What are p -forms?

A p -form is a **totally anti-symmetric** covariant tensor:

$$\omega_{\mu_1 \dots \mu_p} = \omega_{[\mu_1 \dots \mu_p]} .$$

In D -dimensions, the number of degrees of freedom of a **massive p -form** is

$$\text{degrees of freedom} = \frac{(D-1)!}{(D-1-p)!p!} .$$

C. Germani and A. Kehagias, J. Cosmol. Astropart. Phys. 2009, 28 (2009)

Part of the section is based on Morais, B.L, Kumar, Marto and Tavakoli, Phys. Dark Univ. 15, 7 (2017) [arXiv:1608.01679 [gr-qc]]

In a 4-dimensional space-time:

- $p = 0$ (scalar field) \Rightarrow 1 degree of freedom
- $p = 1$ (vector field) \Rightarrow 3 degrees of freedom
- $p = 2 \Rightarrow$ 3 degrees of freedom
- $p = 3 \Rightarrow$ 1 degree of freedom

\Rightarrow The scalar field and the 3-form are the only ones compatible with a homogeneous and isotropic universe (in an easy way).

The 3-form action

- We will consider the following action for a **massive 3-form**, $A_{\mu\nu\rho}$, **minimally coupled** to gravity

$$S^A = \int d^4\mathbf{x} \sqrt{|\det g_{\mu\nu}|} \left[-\frac{1}{48} F^{\mu\nu\rho\sigma} F_{\mu\nu\rho\sigma} - V(A^{\mu\nu\rho} A_{\mu\nu\rho}) \right].$$

- The strength tensor, a 4-form, is defined through the exterior derivative: $F_{\mu\nu\rho\sigma} \equiv 4\nabla_{[\mu} A_{\nu\rho\sigma]}$
- The **equation of motion**, obtained from variation of S^A , is

$$\nabla_{\sigma} F^{\sigma}{}_{\mu\nu\rho} - 12 \frac{\partial V}{\partial (A^2)} A_{\mu\nu\rho} = 0$$

- \Rightarrow a massless 3-form is equivalent to a **cosmological constant**

3-form Cosmology

We consider a **homogeneous and isotropic universe** described by the Friedmann-Lemaître-Robertson-Walker line element

$$ds^2 = -dt^2 + a^2(t)\gamma_{ij}dx^i dx^j .$$

t - cosmic time, $\{\dot{}\} = d\{\}/dt$

a - scale factor

x^i - comoving spatial coordinates (roman indices run from 1 to 3).

Only the **purely spatial components** of the 3-form are dynamical:

$$A_{0ij} = 0 , \quad A_{ijk} = a^3(t)\chi(t)\epsilon_{ijk} .$$

3-form Cosmology: background equations

⇒ Friedmann Equation

$$3H^2 = \kappa^2 \rho_\chi = \kappa^2 \left[\frac{1}{2} (\dot{\chi} + 3H\chi)^2 + V(\chi^2) \right].$$

⇒ Raychaudhuri equation

$$\dot{H} = -\frac{\kappa^2}{2} (\rho_\chi + P_\chi) = -\frac{\kappa^2}{2} \chi \frac{\partial V}{\partial \chi}.$$

A 3-form can show **phantom-like behavior** if $\partial V / \partial \chi^2 < 0$.

⇒ Equation of motion

$$\ddot{\chi} + 3H\dot{\chi} + 3\dot{H}\chi + \frac{\partial V}{\partial \chi} = 0.$$

3-form Cosmology: evolution of χ -1-

Combining the Raychaudhuri equation and the equation of motion for χ :

$$\ddot{\chi} + 3H\dot{\chi} + \left(1 - \frac{\chi^2}{\chi_c^2}\right) \frac{\partial V}{\partial \chi} = 0.$$

The **static solutions** are:

- the **critical points** of the potential: $\frac{\partial V}{\partial \chi} = 0$,
- the limiting points: $\chi = \pm\chi_c$.

Once inside the interval $[-\chi_c, \chi_c]$, the field χ evolves towards a **local minimum of V** .

3-form Cosmology: evolution of χ -2-

- Independently of the shape of a regular potential, in absence of DM interaction, the 3-form decays rapidly towards the interval

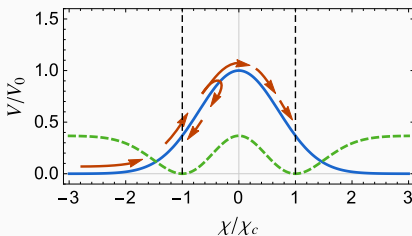
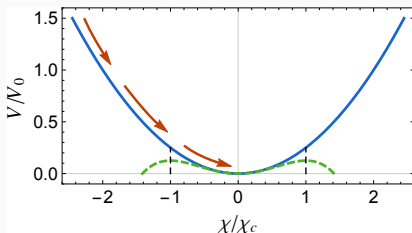
$[-\chi_c, \chi_c]$ Koivisto and Nunes PLB [arXiv:0907.3883], idem PRD [arXiv:0908.0920]

- In an expanding Universe, once inside the interval $[-\chi_c, \chi_c]$, the 3-form will end up in one of the minima of the potential (notice $V_{\text{eff}} \neq V$).

- If the 3-form stops at the limits of this interval:

$$\chi = \pm\chi_c \quad \text{and} \quad \dot{\chi} = 0$$

- \rightarrow Universe heads towards a LSBR event ($\chi_c = \sqrt{2/3\kappa^2}$)



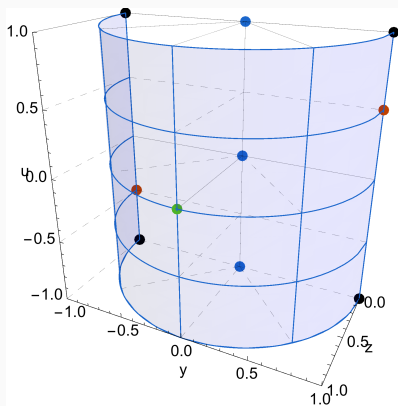
3-forms & with a Gaussian potential: a dynamical system approach

Using a Dynamical Systems representation Morais et al PofDU [arxiv:1608.01679]; BL et al, JCAP

[arXiv:1611.03100]

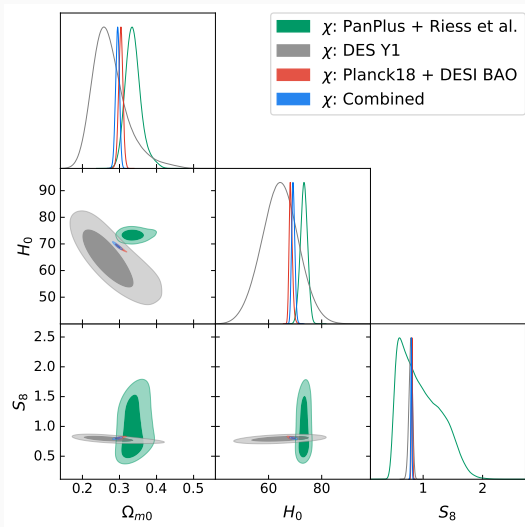
$$u = (\pi/2) \arctan(\chi/\chi_c) \quad y = (\dot{\chi} + 3H\chi)/(3H\chi_c) \quad z = \sqrt{\kappa^2 V/3H^2}$$

- Three **matter era** points:
two repulsive - $(\pm 1, 0, 0)$
one saddle - $(0, 0, 0)$
- One potential dom. **de Sitter**
point: saddle - $(0, 0, 1)$
- Two **LSBR event** points:
attractor - $(\pm 1/2, \pm 1, 0)$
- Four **unphysical** points:
saddles - $(\pm 1, \pm 1, 0)$

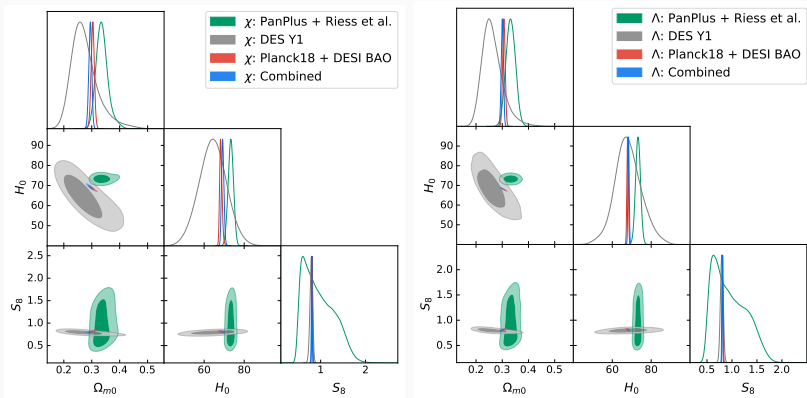


Fixed points in the non-interacting case

Fitting the model with a Gaussian potential-1-

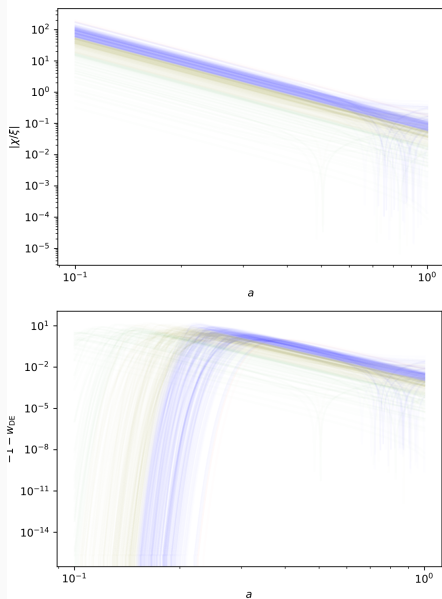


Comparing the model to LCDM

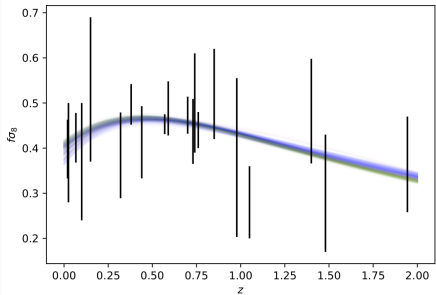
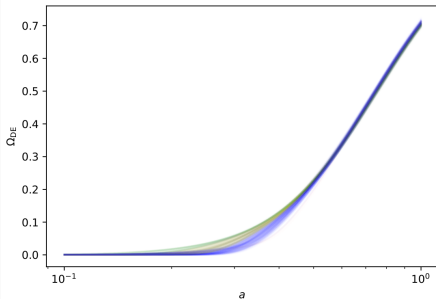


C.G. Boiza, M.B.-L, H.-W. Chiang and P. Chen work in progress (2025)

Fitting the model with a Gaussian potential-2-



Fitting the model with a Gaussian potential-3-



Fitting the model with a Gaussian potential-4-

	CMB	+ BAO	+ SNe	+ low-z	+ DES Y1
$10^4 \Omega_b h^2$	22.19 ± 0.13	22.29 ± 0.12	22.26 ± 0.12	22.34 ± 0.12	22.38 ± 0.12
$10^4 \Omega_c h^2$	119.7 ± 1.0	118.26 ± 0.81	118.56 ± 0.79	117.80 ± 0.76	117.27 ± 0.72
$10^9 \theta_{MC}$	1040.77 ± 0.25	1040.94 ± 0.24	1040.91 ± 0.24	1041.01 ± 0.24	1041.05 ± 0.24
$\ln(10^{10} A_s)$	3.037 ± 0.014	3.044 ± 0.014	3.043 ± 0.014	3.047 ± 0.014	3.046 ± 0.014
n_s	0.9636 ± 0.0040	0.9672 ± 0.0036	0.9665 ± 0.0036	0.9685 ± 0.0036	0.9693 ± 0.0036
τ_{reio}	0.0524 ± 0.0071	0.0571 ± 0.0071	0.0562 ± 0.0070	0.0587 ± 0.0071	0.0589 ± 0.0071
H_0	67.24 ± 0.46	67.89 ± 0.36	67.76 ± 0.35	68.12 ± 0.34	68.36 ± 0.32
Ω_{m0}	0.3154 ± 0.0064	0.3064 ± 0.0048	0.3082 ± 0.0047	0.3034 ± 0.0044	0.3003 ± 0.0042
σ_8	0.8077 ± 0.0055	0.8064 ± 0.0056	0.8067 ± 0.0056	0.8061 ± 0.0057	0.8041 ± 0.0055
S_8	0.828 ± 0.011	0.8149 ± 0.0090	0.8176 ± 0.0090	0.8107 ± 0.0087	0.8044 ± 0.0080
DIC	5497.90 \pm 0.12	5507.21 \pm 0.37	6209.34 \pm 0.14	6217.77 \pm 0.43	6477.38 \pm 0.28
WAIC	5499.09 \pm 0.50	5507.85 \pm 0.18	6210.36 \pm 0.21	6218.68 \pm 0.21	6481.16 \pm 0.22
$-\ln B$	5499.3 \pm 1.1	5508.13 \pm 0.73	6210.51 \pm 0.44	6219.1 \pm 1.4	6479.9 \pm 1.2

Table 2. Mean and standard deviation of cosmological parameters, late-time observables, and statistical probes for Λ CDM model. From left to right are gradually larger datasets that progressively add in datasets of CMB, BAO, etc., as defined in section 4.1.

	CMB	+ BAO	+ SNe	+ low-z	+ DES Y1
$10^4 \Omega_b h^2$	22.18 ± 0.13	22.26 ± 0.13	22.24 ± 0.12	22.25 ± 0.14	22.30 ± 0.13
$10^4 \Omega_c h^2$	119.7 ± 1.1	118.75 ± 0.93	118.96 ± 0.86	118.89 ± 0.96	118.46 ± 0.98
$10^9 \theta_{MC}$	1040.77 ± 0.25	1040.88 ± 0.24	1040.86 ± 0.24	1040.88 ± 0.25	1040.90 ± 0.23
$\ln(10^{10} A_s)$	3.036 ± 0.014	3.042 ± 0.014	3.040 ± 0.014	3.038 ± 0.014	3.037 ± 0.015
n_s	0.9638 ± 0.0040	0.9663 ± 0.0037	0.9657 ± 0.0036	0.9661 ± 0.0038	0.9666 ± 0.0039
τ_{reio}	0.0520 ± 0.0072	0.0554 ± 0.0072	0.0543 ± 0.0071	0.0535 ± 0.0071	0.0532 ± 0.0081
$\log_{10}(\xi/M_P)$	1.6	1.6	1.7	1.7	1.7
$(KE_s + V_0)/\rho_{DE,0}$	1.0000 ± 0.0021	1.0002 ± 0.0027	1.0000 ± 0.0017	1.0004 ± 0.0020	1.0006 ± 0.0038
$\log_{10}(\sigma_8^2 \chi_s / \xi)$	$-2.3^{+0.6}$	$-1.6^{+0.3}$	$-1.86^{+0.09}$	$-1.27^{+0.28}$	$-1.23^{+0.27}$
$(\dot{\chi}_i + 3H_i \chi_i) \rho_{crit, h=1}^{-1/2}$	0.01 ± 0.15	0.01 ± 0.17	0.002 ± 0.063	-0.005 ± 0.073	0.01 ± 0.14
H_0	$67.51^{+0.88}_{-0.090}$	$68.29^{+0.96}_{-0.61}$	$68.02^{+0.45}_{-0.46}$	68.99 ± 0.59	69.28 ± 0.59
Ω_{m0}	$0.3116^{+0.0060}_{-0.0072}$	0.3030 ± 0.0059	0.3062 ± 0.0052	0.2980 ± 0.0053	0.2946 ± 0.0052
σ_8	$0.8076^{+0.0063}_{-0.0063}$	0.8080 ± 0.0069	0.8061 ± 0.0064	0.8098 ± 0.0073	0.8091 ± 0.0065
S_8	$0.822^{+0.013}_{-0.013}$	0.8120 ± 0.0093	0.8144 ± 0.0089	0.8070 ± 0.0088	0.8018 ± 0.0084
DIC	5498.84 \pm 0.18	5507.37 \pm 0.30	6209.55 \pm 0.22	6216.47 \pm 0.42	6476.1 \pm 1.1
WAIC	5499.41 \pm 0.03	5507.90 \pm 0.14	6210.12 \pm 0.15	6217.18 \pm 0.74	6479.18 \pm 0.00
$-\ln B$	5499.9 \pm 1.4	5507.66 \pm 0.96	6212.9 \pm 1.9	6217.94 \pm 0.91	6475.61 \pm 0.06
Δ DIC	0.94 ± 0.24	0.15 ± 0.53	0.21 ± 0.28	-1.30 ± 0.66	-1.3 ± 1.2
Δ WAIC	0.32 ± 0.59	0.05 ± 0.26	-0.25 ± 0.29	-1.50 ± 0.79	-1.98 ± 0.26
$-\Delta \ln B$	0.6 ± 1.9	-0.46 ± 0.86	2.4 ± 2.0	-1.2 ± 2.0	-4.3 ± 1.4

Table 3. Mean and standard deviation of cosmological parameters, late-time observables, and statistical probes for the 3-form dark energy model in section 2. From left to right are gradually larger datasets of CMB, CMB + BAO, CMB + BAO + SNe, etc., as defined in section 4.1. Δ ICs are with respect to Λ CDM model presented in table 2. For parameters not following Gaussian distribution we provide the median and 68% lower and upper bounds (if valid) instead, with color coding for how heavy the tail is (red for short tail, black for Gaussian, blue for exponential, and cyan for long tail.) For single-sided distributions we report the modal and the single-sided 68% bound instead.

Modified theory within $f(Q)$ gravity

Geometry of Spacetime: Metricity vs Non-Metricity

- We assume a space-time endowed with a metric $g_{\mu\nu}$ and a symmetric connection $\Gamma_{\mu\nu}^{\lambda}$, i.e. **NO** torsion:
- What is metricity, and how does it differ from non-metricity?

Metric Compatibility

$$\nabla_{\lambda} g_{\mu\nu} = 0$$

The covariant derivative of the metric tensor vanishes, meaning the length of vectors is preserved under parallel transport. Then the connection is uniquely determined by the metric and is given by the Levi-Civita connection.

Non-Metricity Tensor

$$Q_{\lambda\mu\nu} = \nabla_{\lambda} g_{\mu\nu} \neq 0$$

Represents the failure of the connection to preserve the metric under parallel transport. Therefore, the length of a vector may change.

Curvature of Spacetime: Metricity vs Non-Metricity

- The scalar curvature of a space-time endowed with a metric $g_{\mu\nu}$ and a symmetric connection $\Gamma_{\mu\nu}^\lambda$ can be written as:

$$R(\Gamma) = \mathcal{R}(\{\}) + Q + \text{surface terms},$$

where

$$Q := -\frac{1}{4} Q_{\alpha\mu\nu} Q^{\alpha\mu\nu} + \frac{1}{2} Q_{\alpha\mu\nu} Q^{\mu\alpha\nu} + \frac{1}{4} Q_\alpha Q^\alpha - \frac{1}{2} Q_\alpha \tilde{Q}^\alpha$$
$$Q_\alpha := Q_{\alpha\mu}{}^\mu \quad \tilde{Q}_\alpha := Q_{\mu\alpha}{}^\mu .$$

- For a vanishing $R(\Gamma)$ a theory with Lagrangian density linear on $\mathcal{R}(\{\})$, is equivalent to a theory with Lagrangian density linear in Q .
- The former statment does not apply to $f(\mathcal{R}(\{\}))$ and $f(Q)$ because of the surface term.
- This gives rise to $f(Q)$ gravity as a new avenue of exploration, particularly from a phenomenological perspective, for example.

- The gravitational action:

$$S = \int d^4x \sqrt{-g} [f(Q) + \mathcal{L}_M].$$

- The equations of motion are deduced by **varying** the action with respect to **the metric and the connection**.
- The **energy momentum** tensor for matter is **conserved**.

J. Beltrán Jiménez, L. Heisenberg, and T. S. Koivisto, arXiv:1803.10185 (proposer of the theories)

R. Lazkoz, F. S. N. Lobo, M. Ortiz-Baños, and V. Salzano, arXiv:1907.13219 (among the first cosmological fits)

FLRW cosmology in $f(Q)$ gravity

- The metric:

$$ds^2 = -N(t)dt^2 + a^2(t) [dr^2 + r^2 (d\theta^2 + \sin^2 \theta d\phi^2)] ,$$

- The connection must be consistent with the symmetries of the FLRW metric; it should also be symmetric and satisfy the flatness condition, i.e. $R(\Gamma) = 0$.
- There are three possible connections that satisfy the above criteria, highlighting the richness of the theory.
- From now on, we shall adopt the simplest choice for the connection, maintaining the FLRW metric in its standard form.

F. D'Ambrosio, L. Heisenberg, and S. Kuhn, arXiv:2109.04209, I. Ayuso, M. B.-L., C.-Y. Chen, X. Y. Chew, K. Dialektopoulos, Y. C.

Ong, arXiv:2109.04209

Suitable $f(Q)$ models for cosmology-1-

- Friedmann and Raychaudhuri equations:

$$6f_Q H^2 - \frac{1}{2}f = \rho_m \quad (12H^2 f_{QQ} + f_Q)\dot{H} = -\frac{1}{2}(\rho_m + p_m).$$

- The conservation equation:

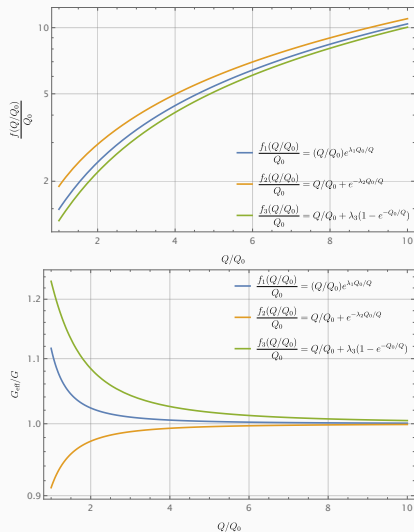
$$\dot{\rho}_m + 3H(\rho_m + p_m) = 0.$$

- Three potential candidates:

$$\begin{aligned} f_1(Q) &= Q \exp(\lambda Q_0/Q), \\ f_2(Q) &= Q + Q_0 \exp(-\lambda Q_0/Q), \\ f_3(Q) &= Q + \lambda Q_0 [1 - \exp(-Q_0/Q)]. \end{aligned}$$

- All these models give rise to late-time acceleration.
- The first model previously analysed in [F. K. Anagnostopoulos, S. Basilakos and E. N. Saridakis, arXiv:2104.15123 \[gr-qc\]](#).

Suitable $f(Q)$ models for cosmology-2-

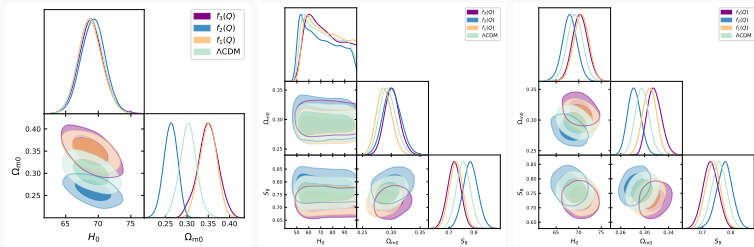


C.G. Boiza, M. Petronikolou, M.B.-L, E. N. Saridakis, arXiv:2505.18264

Observational constraints

- The analysis is performed for three different combinations of datasets:
 - **Combination I:** Cosmic chronometers (CC), supernovae (SN), and gamma-ray bursts (GRB);
 - **Combination II:** Baryon acoustic oscillations (BAO) and redshift-space distortions (RSD);
 - **Combination III:** Full combination (CC + SN + GRB + BAO + RSD).

Fitting the model-1-



C.G. Boiza, M. Petronikou, M.B.-L. and E. N. Saridakis: arXiv:2505.18264

Fitting the model-2-

Model	H_0	Ω_{m0}	r_d	S_8	ΔAIC
CC + SN + GRB					
$f_3(Q)$	68.91 ± 1.90	0.3495 ± 0.0241	–	–	–0.23
$f_2(Q)$	69.20 ± 1.84	0.2616 ± 0.0160	–	–	1.67
$f_1(Q)$	68.76 ± 1.85	0.3497 ± 0.0200	–	–	0.17
ΛCDM	68.89 ± 1.86	0.3027 ± 0.0198	–	–	–
BAO + RSD					
$f_3(Q)$	–	0.3015 ± 0.0133	–	0.7206 ± 0.0285	2.63
$f_2(Q)$	–	0.3013 ± 0.0156	–	0.7856 ± 0.0294	0.51
$f_1(Q)$	–	0.2877 ± 0.0132	–	0.7270 ± 0.0263	2.30
ΛCDM	–	0.2937 ± 0.0142	–	0.7567 ± 0.0279	–
CC + SN + GRB + BAO + RSD					
$f_3(Q)$	70.31 ± 1.71	0.3163 ± 0.0117	147.09 ± 3.49	0.7280 ± 0.0270	6.08
$f_2(Q)$	68.01 ± 1.67	0.2827 ± 0.0109	147.62 ± 3.46	0.7773 ± 0.0280	5.19
$f_1(Q)$	70.56 ± 1.69	0.3080 ± 0.0113	146.98 ± 3.43	0.7361 ± 0.0264	8.90
ΛCDM	69.15 ± 1.73	0.2958 ± 0.0115	147.33 ± 3.57	0.7580 ± 0.0271	–

TABLE III: Mean values and standard deviations of the cosmological parameters obtained for each $f(Q)$ model, namely $f_1(Q) = Q \exp(\lambda Q_0/Q)$, $f_2(Q) = Q + Q_0 \exp(-\lambda Q_0/Q)$, and $f_3(Q) = Q + \lambda Q_0[1 - \exp(-Q_0/Q)]$, and for ΛCDM paradigm, under the three different dataset combinations considered in this work: **Combination I** (CC + SN + GRB), **Combination II** (BAO + RSD), and **Combination III** (CC + SN + GRB + BAO + RSD). The parameter S_8 is derived from the fitted value of σ_8 . The last column shows the AIC difference, $\Delta\text{AIC} \equiv \text{AIC}_{f(Q)} - \text{AIC}_{\Lambda\text{CDM}}$, quantifying the statistical preference relative to the ΛCDM model.

Fitting the model-3-

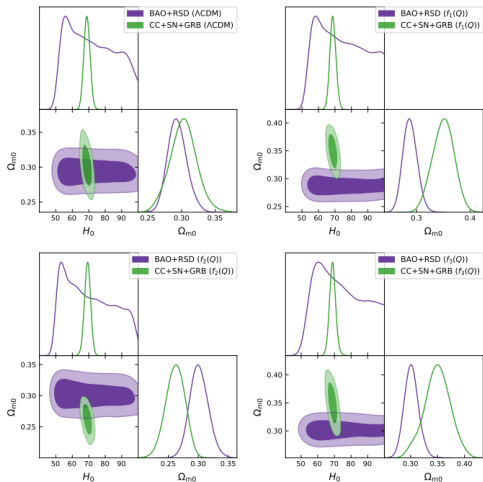


FIG. 3: Comparison of the two-dimensional posterior distributions obtained from Combination I (CC + SN + GRB) and Combination II (BAO + RSD) for each model separately. The contours correspond to the 68% and 95% confidence levels (C.L.). The top-left panel shows the results for Λ CDM scenario, which displays excellent agreement between the two dataset combinations. The remaining panels correspond to Models 1 (top-right), 2 (bottom-left), and 3 (bottom-right), where a clear tension between the two combinations emerges in the $\Omega_{m0} - H_0$ plane. These internal inconsistencies contribute to the poorer global fits obtained by the $f(Q)$ models when all datasets are combined.

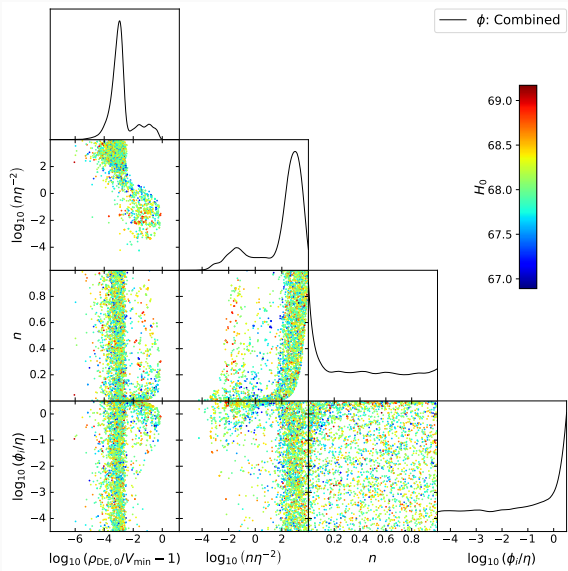
Conclusions

Conclusions

- We have introduced an axion-like model that mimics a dynamical cosmological constant through a tracking regime, providing a fit as good as Λ CDM while also addressing the coincidence problem.
- We have described DE through a field encoded on a DE KGB model or a 3-form field. The 3-form field with a Gaussian potential can allviate the H_0 tension.
- We have also discussed several $f(Q)$ models, highlighting the impact that G_{eff} can have on certain cosmological observables, and how useful these models can be in alleviating the H_0 and S_8 tensions.
- We are currently analysing certain extensions of the Λ_s CDM model (O. Akarsu, S. Kumar, E. Özüiker, J. A. Vázquez, arXiv:2108.09239), and the initial fits appear promising (in collaboration with B. Ibarra, arXiv:2506.12139, arXiv:2506.18992).
- In a different work (M. Benetti, P. Morilla, M-B.-L., S. Capozziello, arXiv:2507.XXXX), we are analysing some special cases related to the mGCG.

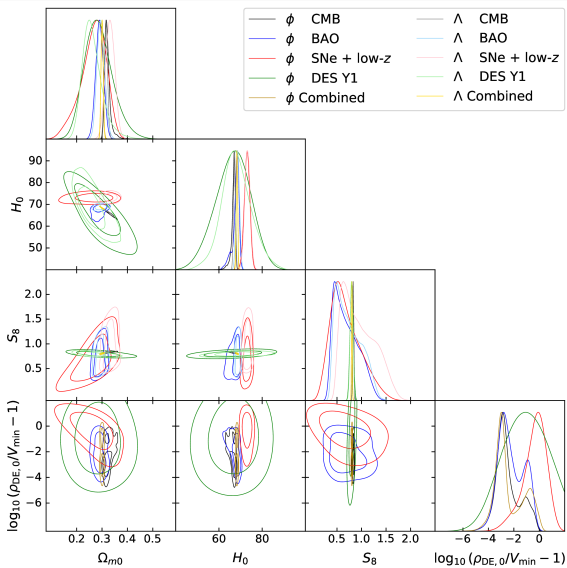
Thank you for your attention !!!

Fitting the model-2-



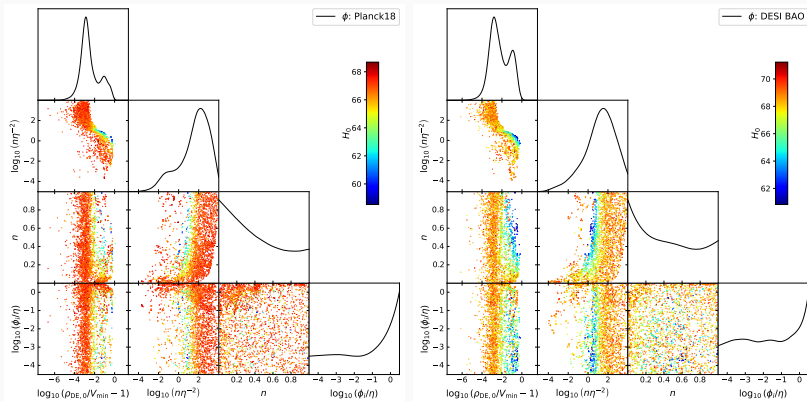
H.-W. Chiang, C.G. Boiza and M.B.-L.: arxiv:2503.04898

Fitting the model-3-



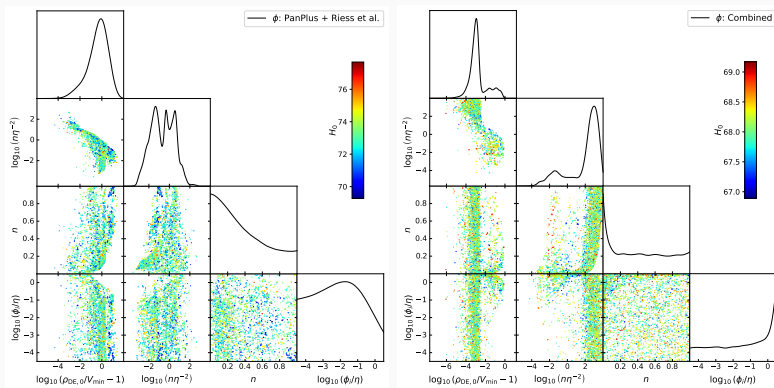
H.-W. Chiang, C.G. Boiza and M.B.-L.: [arxiv:2503.04898](https://arxiv.org/abs/2503.04898)

Fitting the model-4-



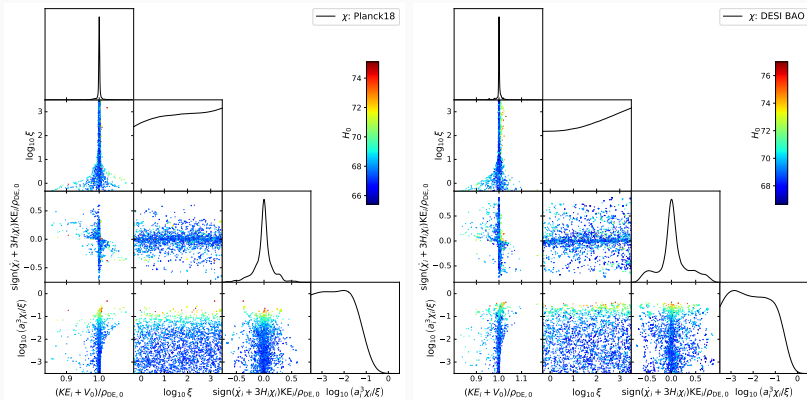
H.-W. Chiang, C.G. Boiza and M.B.-L.: [arxiv:2503.04898](https://arxiv.org/abs/2503.04898)

Fitting the model-5-



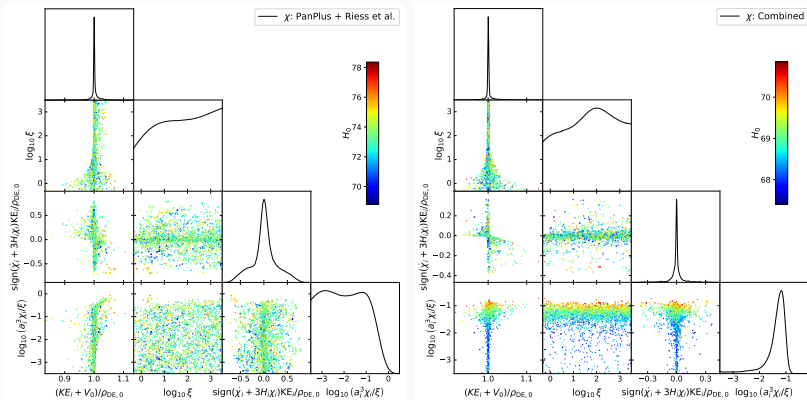
H.-W. Chiang, C.G. Boiza and M.B.-L.: arxiv:2503.04898

Fitting the model with a Gaussian potential-2-



C.G. Boiza, M.B.-L, H.-W. Chiang and P. Chen work in progress (2025)

Fitting the model with a Gaussian potential-3-



C.G. Boiza, M.B.-L, H.-W. Chiang and P. Chen work in progress (2025)

Further consideration with 3-forms from a gravitational point of view

Let me add that 3-forms can be quite interesting for further reasons as:

- They allow naturally for regular BHs ([Bouhmadi-López, Chen, Chew, Ong and Yeom, arXiv: 2005.13260 \[gr-qc\]. Published in EPJC 2021](#))
- They naturally support wormholes without changing the sign of the kinetic energy ([Bouhmadi-López, Chen, Chew, Ong and Yeom, arXiv: 2108.07302 \[gr-qc\]. Published in JCAP 2021](#)).

The Little Sibling of the Big Rip

The **Little Sibling of the Big Rip** (LSBR) is a cosmological event that happens at infinite time and is characterised by

- $a(t \rightarrow \infty) \rightarrow +\infty$,
- $H(t \rightarrow \infty) \rightarrow \infty$,
- $\dot{H}(t \rightarrow \infty) \rightarrow \text{constant}$.

In general, this can be obtained with an equation of state:

$$p = -\rho - A \quad (A > 0).$$

Solving the conservation equation we find $H^2 \propto \log(a)$ and $\dot{H} = (\kappa^2/2)A$ (asymptotically).